Micro-Temperature Sensor based on Optical Whispering Gallery Mode of Fiber Taper-Microsphere Coupling System

Qiulin Ma, Tobias Rossmann and Zhixiong Guo

Department of Mechanical and Aerospace Engineering Rutgers, The State University of New Jersey Piscataway, NJ 08854, USA

ABSTRACT

Miniaturized Whispering Gallery Mode (WGM) temperature sensor has great potentials of high resolution and great on-chip integration capability. This study focuses on the development of this kind of sensor based on the shifting wavelength of the optical resonance due to thermal expansion and thermo-optic effects of a silica microsphere. Excellent linear dependence of the wavelength shift versus temperature rise is observed for three sizes of microspheres (D=90μm, 145μm and 313μm) in small temperature ranges (≤17K) at very low temperatures (113±1K to 173K). By comparing this observation with the results of similar sizes of microspheres of our previous study in near room temperature as well as with a theoretical analysis, a conclusion is drawn that thermal expansion and thermal optic coefficients need to be further studied for microscale silica materials. Ultra high resolution sensing capability as well as potentials of integrated & miniaturized applications of the WGM temperature sensor is discussed. A method is designed to initially characterize the WGM temperature measurement noise level due to self-heating effect of the WGM resonance.

Keywords: Whispering Gallery Mode, Microsphere, Fiber Taper, Temperature Sensor

1. INTRODUCTION

Optical Whispering Gallery Mode (WGM) effects in dielectric micro resonators have been extensively studied over the last several years due to their high quality factors (Q), low mode volumes, and potential use in many areas including cavity quantum electrodynamics[1], laser stabilization[2], micro lasers[3-6], nonlinear optics[7-9], and chemical & biological sensors[10,11]. The WGM's propagate on a circular path around the micro-resonator which can be a disk, a ring, or a sphere, remaining confined in a thin layer beneath the surface. They correspond to electromagnetic waves trapped and resonated in circling orbits just within the surface of the cavity, being continuously totally reflected from the surface. Under these circumstances, the leakage of the light can be extremely low and thus gives very high Q values. The spherical WGM's are by convention characterized in terms of three mode numbers representing the radial, azimuthal, and polar field distributions. The radial part can be described by spherical Bessel functions, the polar field follows spherical harmonics, and the azimuthal field varies sinusoidally. The modes that are mostly confined to the surface of the sphere are usually being excited and used for sensing.

Resonance wavelengths of WGM are determined simply by the size and refractive index of a resonator. A tiny variation of the size and/or refractive index is able to introduce a significant resonance wavelength shift for a given mode. This feature has been broadly studied for use in WGM-based sensors [12, 13]. On the other hand, the material properties of a

Photonic Fiber and Crystal Devices: Advances in Materials and Innovations in Device Applications III, edited by Shizhuo Yin, Ruyan Guo, Proc. of SPIE Vol. 7420, 74200Q · © 2009 SPIE · CCC code: 0277-786X/09/$18 · doi: 10.1117/12.827417

resonator are susceptible to thermal fluctuations caused by either the ambient temperature variation or the absorption of laser energy during the laser scanning or pumping. Thermal expansion and thermo-optic effects are two noticeable properties of material, causing the resonator size and refractive index to change, respectively. Cai et al. [14] found red shifts on the frequency of a single mode in a glass microchip laser when the pump power is increased and quantitatively explained the phenomenon based on thermal expansion effect of the chip material. As stability and continuous operation are critical for use of a micro resonator, Carmen et al. [15] demonstrated a self-stable thermal equilibrium solution for micro cavity-pump system. Recently, Han and Wang [16] proposed qualitatively the use of a surface layer with a negative thermo-optic coefficient to compensate the thermal drift of a resonance frequency in an optical micro resonator.

In this experimental study, low-transmission-loss sub-micrometer waist size fiber taper and high Q microspheres of various sizes (50~500μm) are fabricated from single mode silica fibers for generating optical WGM resonances at wavelengths around 1531nm. Phase match couplings [17] can be made by scanning a microsphere along the fiber taper waist. The WGM resonance wavelength shifts of fused silica microspheres were investigated with well-controlled temperature changes in a very low temperature range (113±1K to 173K), and compared with our previous study of near room temperature sensing[18]. The temperature tuning curves of three microspheres of different sizes are plotted and temperature sensitivities (resonance wavelength shift versus temperature) are extracted through curve fitting. The theoretical temperature sensitivity of the microspheres is analyzed and calculated based on bulk silica material properties. Comparisons and discussions are made between theoretical and experimental results. Lastly, for characterizing the sensor noise level, WGM coupling is made in vacuum for an attempt to expose the effect of laser wavelength drifting and extract out self-heating effect by comparing the WGM continuous shifts with the interference peak shifts of a fiber ring resonator.

2. FABRICATION OF WGM COUPLING SYSTEM

Corning SMF-28 silica fiber is used for microsphere fabrication. It is a standard telecommunication single mode fiber with a core diameter about 8.2μm and cladding diameter about 125μm. The core is slightly doped silica resulting in slightly higher refractive index than the cladding which is made of pure silica. The core takes only a small portion of the whole materials which is good to fabricate microsphere with uniform component distribution. Years of industrial effort have made this kind of fiber with very low attenuation rate of ≤0.22dB/km for telecommunication band 1525-1575nm.

Microspheres (about 50~500μm) are fabricated by melting the tip of a strictly cleaned stripped fiber or fiber taper with oxy-hydrogen flame (2800~3080K) [18]. During the fabrication, once the silica passes the melting point, surface tension shapes the material into a spheroidal form. The sphere glowing hot white is then moved slowly to lower temperature part of the flame to do seconds of annealing which reduces the density variation and allows time for surface variations being smoothed out by surface tension. This technique has been found to produce minimal amount of soot that can spoil the quality of the microsphere. The surface microstructure is also examined with Scanning Electronic Microscopy (SEM) and only nano-scale dips and bumps are observed as an evidence of its super-smoothness [18].

The modes in a WGM microcavity are highly confined and thus are not accessible by free-space beam. Therefore a near-field coupler is required to couple the light in and out of the cavity through evanescent waves. The coupler utilized for this study is a fiber taper. It allows sensitive tuning of the fiber mode propagation constant by controlling the size of

the fiber thickness or scanning the microsphere across different part of the taper waist. It can not only align with the microsphere easily but also efficiently couple the light into and out of the microsphere. The taper is fabricated through a heating and pulling technique as shown in Fig.1. One end of a stripped single mode fiber (Corning SMF-28) is fixed and the other end is pulled with a computerized stepper motor. During the pulling procedure, a hydrogen flame (about 2400K) is used for heating and softening the taper waist. The DFB laser (NEL NLK1556STG) is set to deliver continuous wave light of a constant intensity into the fiber during fabrication and its transmission signal through the taper is dynamically

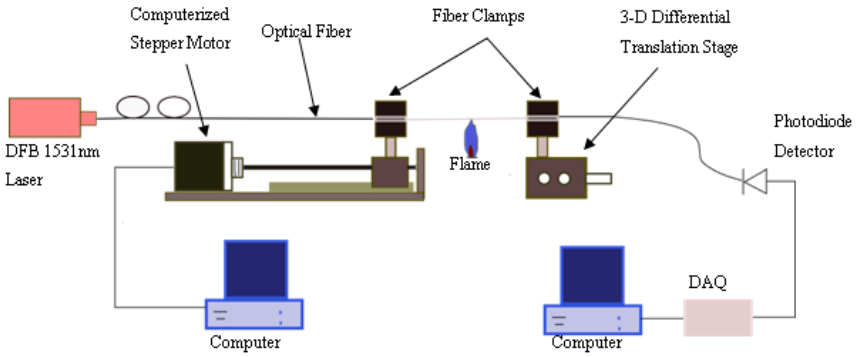

Fig. 1. Setup of the fiber taper fabrication by the technique of heating and pulling.

monitored, making sure negligible transmission loss during the tapering. The waist size of a taper can reach submicron level confirmed by SEM measurement [18]. The adiabatic condition [19] is examined to preserve the propagation of a fundamental mode of light in the tapered region. It is calculated that the transitional tapered region must be longer than 2.51mm to satisfy this condition for our DFB 1531nm laser and SMF-28 fiber, the condition of which all our fabricated fiber tapers have easily met.

3. EXPERIMENTAL SETUP OF WGM TEMPERATURE SENSOR TEST

For very low temperature tests, a cell for enclosing both the WGM coupling system and a thermocouple is constructed with a similar design of our previous near-room temperature sensing study [18] which is shown in Fig.2. It is made of copper for efficient cooling and insulated with fiber glass for keeping low temperature inside. The top cover is made of fiber glass insulated glass slide and is removed in the figure for observing the alignment in the cell. The four

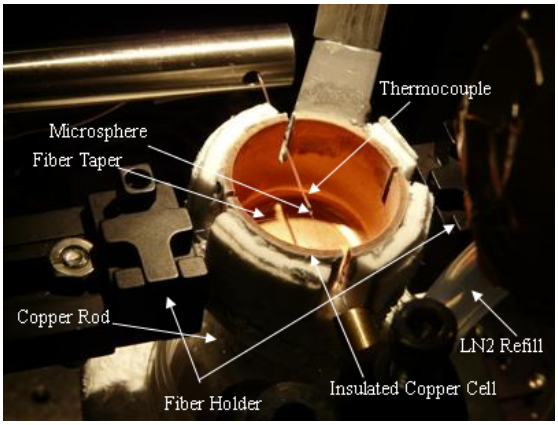

Fig. 2. WGM temperature sensor test alignment in very low temperature (110K~170K) test cell.

accessible slits are sealed as much as possible during test. The copper cell is about 1 inch in diameter and 1 inch in height. A copper rod about 1 inch in diameter and 2.5 inch in height is attached to the bottom of the cell and almost fully dipped into liquid nitrogen (LN_2) for cooling the cell. Liquid nitrogen is continuously refilled into the container and the temperature inside the cell can be cooled down to around 110K measured by the thermocouple. The temperature inside stays at around 110K for about nine minutes before the LN_2 level falls below the copper rod. Then the temperature increases slowly as shown in Fig.3, which is a typical temperature history of every test. It takes about 20 minutes to

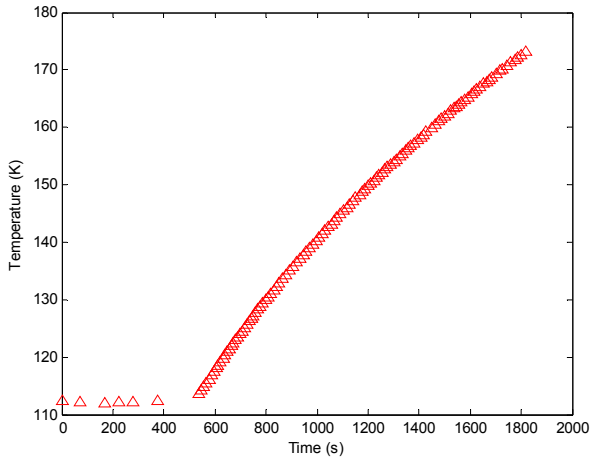

Fig. 3. A typical temperature history of the low temperature sensor test.

increase about 60K, averagely around 20s/K. The thermal response times of both the silica microspheres and the thermocouple bead can be estimated using the lumped capacity analysis of heat transfer [20]. For example, the thermal relaxation time of a silica microsphere of 450μm in diameter is about 0.9sec. The smaller the microsphere, the shorter is the thermal response time. Thus, the microsphere and thermocouple are able to follow and reflect the real temperature in the cell. And if they are placed close enough to each other, they measure approximately the same temperature.

The alignment and measurement system is shown in Fig.4. The DFB 1531nm laser is tuned by a 'saw shape' injection current and launched into the optical fiber taper. The fiber taper is aligned through the two narrow slits of the cell and

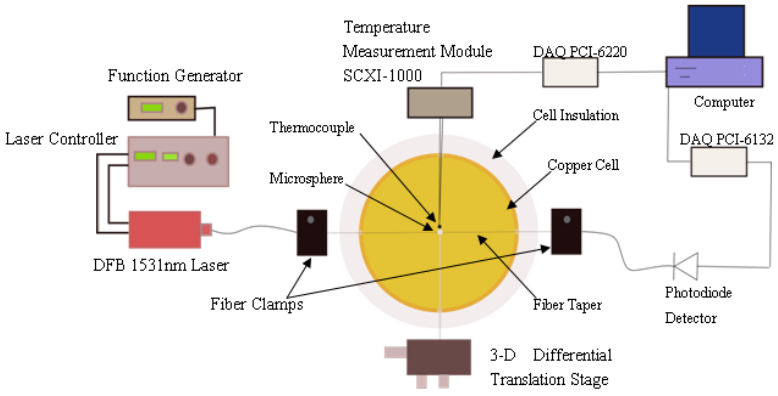

Fig. 4. Diagram of the WGM Temperature Sensor Test Setup.

held by two fiber clamps, while the microsphere and thermocouple are put into the cell through the other two slits as shown in both Fig.2 and 4. The microsphere is precisely positioned by a 3-D differential translation stage to couple with the fiber taper in the cell. The microsphere-taper coupling is observed and managed under a stereo-microscope (Zeiss SV8). The transmission signal is detected by a photodiode detector (Thorlabs PDA400) and recorded by a computer equipped with a high sampling rate DAQ card (National Instrument PCI-6132) for tracking WGM peak positions accurately. The thermocouple is positioned about 0.1mm away from the microsphere to track the temperature change around the microsphere. The temperature signal is acquired by a high accuracy DAQ card (PCI-6220) in the same computer. The two data acquisitions for temperature and WGM resonance spectrum are synchronized in LabView.

4. THEORETICAL ANALYSIS

Assuming a WGM propagates as a k^{th} polygon in a microsphere and there are m EM field maxima on the circumference which is much longer than the resonance wavelength, we have

$$kD\sin\frac{\pi}{k} = m\frac{\lambda}{n} \quad , \tag{1}$$

where λ is the resonance wavelength in vacuum, D and n are the diameter and refractive index of the resonator respectively. Since k is very large, we have

$$\pi D = m\frac{\lambda}{n} . \tag{2}$$

Taking a variation of (2), we have

$$\frac{dn}{n} + \frac{dD}{D} = \frac{d\lambda}{\lambda} . \tag{3}$$

Assume a linear thermal expansion and thermo-optic effects [21], we have

$$\frac{dD}{D} = \alpha dT \quad \text{and} \quad \frac{dn}{n} = \beta dT , \tag{4}$$

where α and β are the thermal expansion coefficient and thermo-optic coefficient, respectively. Thus the temperature sensitivity of a microsphere is

$$\frac{d\lambda}{dT} = (\alpha + \beta)\lambda . \tag{5}$$

α and β can be assumed as weak functions of temperature provided that the temperature tuning range is small (≤17K in this study).

5. RESULTS AND DISCUSSION OF WGM TEMPERATURE SENSOR

The wavelength versus injection current for laser tuning is measured by an optical spectrum analyzer (ANDO AQ6317B). A significant WGM resonance that appears in each tuning is selected for measuring the resonance shift against temperature. Fig.5 shows three measured WGM spectra from the microsphere of 313μm in diameter for demonstration of the shift during very low temperature sensing. The Q value of the microsphere is 7×10^6 from the dip indicated in the figure. Microspheres with diameter of 90, 145 and 313, respectively, are tested in a very low temperature range from 113±1K to 173K. Linear curve fittings are done for four sections (≤17K each) of temperature change for the very low

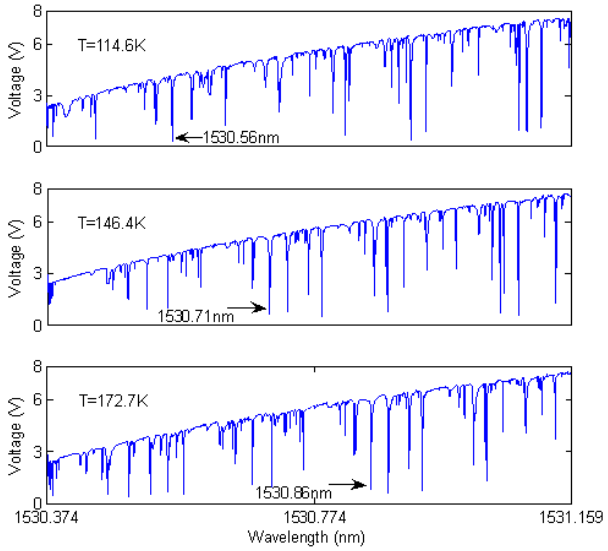

Fig. 5. Transmission spectra of the microsphere of 313μm in diameter (Q=7×10^6) at three different temperature stages during very low temperature sensing test.

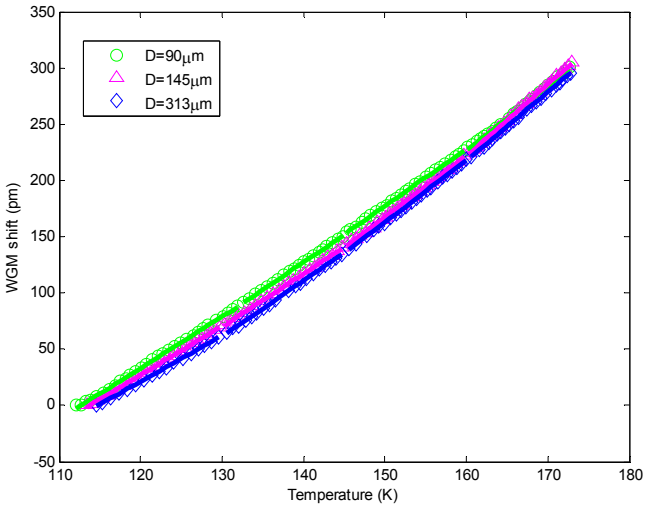

Fig. 6. Linear fitting curves of WGM resonance wavelength shifts against temperature for tested microspheres in smaller temperature ranges (≤17K) in the very low temperature range (113±1K to 173K).

temperature tests as shown in Fig.6. In previous near-room temperature (297K~307K) study [18] with three similar sizes (D=83μm, 146μm and 290μm, respecitvely) of microspheres, the theoretical values of temperature sensitivities of larger sphere (D=290μm) calculated from equation (5) matches the measured sensitivities very well with a difference within 0.6% [18]. However, the measured temperature sensitivities tend to be bigger than the analytical values when microsphere size gets smaller. The measured sensitivity is about 32% more than the analytical value for the microsphere of 83μm in diameter. The problem is most likely from α and β values in analysis which are the properties of bulk materials. The

geometrics interpretation should not fail, since the equator circumference of this sphere is still much longer than the resonance wavelength. Further studies for thermal expansion and thermo-optic effect in micro/nano scale materials are needed. However, the linearity is still good for smaller microsphere (<150μm) and the sensitivity is relatively bigger which is also a preferable change for developing miniaturized temperature sensors [18]. The tested low temperature ranges is much longer. The WGM shift does not change linearly with temperature any more in this whole temperature range as can be seen in Fig.6. However, the linear curve fitting still works great for smaller temperature ranges 113K~130K, 130K~145K, 145K~160K and 160~173K, which are sectioned for comparing the sensitivities at different temperature levels. The correlation coefficient is all above 0.9992 and the errors of the measured sensitivities from the fitting are less than ±0.06pm/K. It is know from reference [22] that β =4.27×10^{-6}/K, 4.64×10^{-6}/K, 5.02×10^{-6}/K and 5.39×10^{-6}/K averagely and respectively for the four different temperature ranges. The related thermal expansion coefficients are -0.37×10^{-6}/K, -0.26×10^{-6}/K, -0.16×10^{-6}/K and -0.06×10^{-6}/K, respectively [24]. The thermal optic coefficient is still the dominant factor. The mean temperature is taken for each of the temperature range to correlate with the related sensitivity. Fig.7 shows the theoretical sensitivities by using α and β values and the measured sensitivities in the four temperature

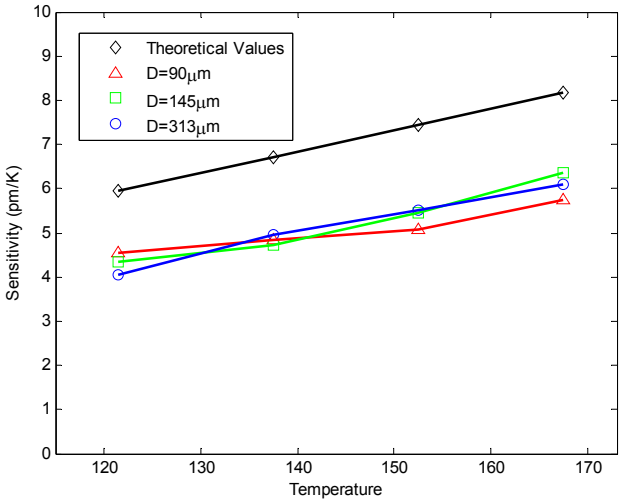

Fig. 7. Theoretical sensitivities and measured sensitivities of the microspheres in very low temperatures

ranges for the three different sizes of microspheres. The measured sensitivities increase at a similar rate as the theoretical values, although a difference about between 22%~32% exists between theory and experiment. This is still most likely due to that α and β values are bulk materials properties. They may significantly changes when the materials shrink down to sizes of the microspheres at the tested very low temperatures.

5. MERITS OF THE WGM TEMPERATURE SENSOR

The WGM-based temperature sensors are basically frequency-modulated (FM) sensors which is inherently more sensitive than an intensity-modulated (IM) sensor like a thermocouple. The linewidth of WGM resonance, $\delta\lambda$, and the sensor's performance can be characterized by the resonator's quality factor, Q= $\lambda/\delta\lambda$. A high Q is essential to resolve a small resonance wavelength change $\Delta\lambda$ associated with the temperature change, since the sensor detection limit is set by how well one can locate a resonance wavelength λ. One can locate a resonance wavelength change to $\delta\lambda/100$ with

ease [25]. Usually a Q=10^8 is easily achievable by optimizing the microsphere-fiber taper WGM coupling. The associated detectable resonance wavelength shift is 1.56×10^{-4}pm around 1531nm wavelength. If an approximate WGM temperature sensitivity, 14 pm/K, in near room temperature is used, the minimum resolvable temperature will be 1.11×10^{-5} K. This is an amazingly high temperature resolution based on a theoretical estimate. However, in real applications the effect of the resonant light heating the resonator (self-heating) needs to be considered for characterizing the noise level.

In addition to the ultra high resolution, WGM micro sensors have great potentials in on-chip temperature monitoring which is currently a challenging task [26] because a chip may be easily overheated to function incorrectly or to receive a fatal damage without a proper temperature monitoring and thermal solution. Nevertheless, integrating a common type of sensors (such as thermodiodes, thermistors or thermocouples) into a chip is technically difficult. However, WGM sensors can be easily fabricated and integrated into other electro-optical systems using existing microelectronics techniques [27]. Further, the thermo-optic effect can be dominant as in the silica resonators and this will minimize the mechanical stress induced to the chip by thermal expansion. Recent developments in micro fluidics and lab-on-a-chip devices have also raised the challenge of whole-chip (liquid and substrate) temperature measurement [28]. Traditional embedded thermocouples have been used for micro fluidics applications. However, measurements are limited to single locations unless complex fabrication and data acquisition are implemented for multiple thermocouples [29, 30]. It is possible that arrays of WGM sensors be fabricated on a chip and coupled with just one waveguide to monitor temperatures at different locations.

6. CHARACTERAZATION OF WGM TEMPERATURE SENSOR NOISE LEVEL

As stated above, the temperature measurement resolution is not solely determined by Q value of the microsphere. The noise due to self-heating effect has to be considered in real applications. In order to extract the tiny WGM resonance wavelength drift induced by self-heating, the coupling system needs to be placed in vacuum to avoid transferring of heat with surrounding medium. In addition, the laser drifting & tuning properties have to be tracked simultaneously with a WGM resonance since a shift is measured relative to the start point of each laser wavelength tuning period. The experiment setup is shown in Fig.8. The WGM coupling is made in a vacuum chamber and can be adjusted by a

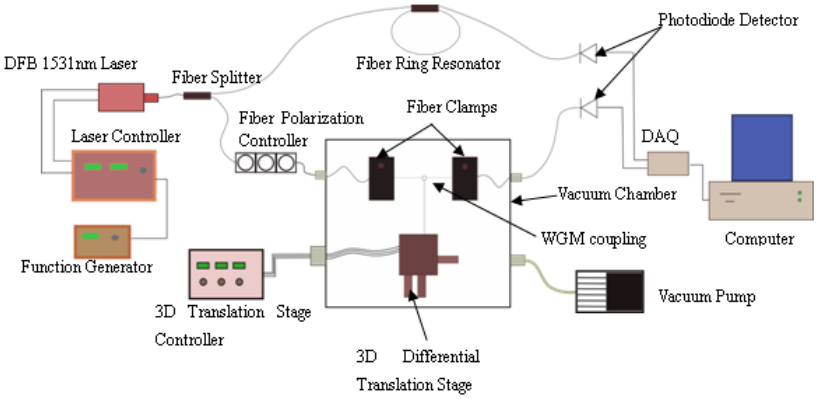

Fig. 8. Experiment setup for tracing WGM self-heating effect.

3D-translation stage controller (MDT 693A, Thorlabs) outside the chamber with a vacuum electrical feedthrough.

Since WGM coupling is polarization dependent, a fiber polarization controller (FPC561, Thorlabs) is employed to further adjust and optimize the coupling in vacuum. The fiber is fed into the chamber with the technique developed by E. Abraham et al [31]. The pressure inside the chamber can be pumped down to 0.6 torr. The tunable 1531nm laser is split into two fibers, one goes to the chamber for WGM coupling, the other one goes to a fiber ring resonator (FBR) which is essentially a Fabry-Perot interferometer (or Etalon). This FBR is used to track the laser wavelength drifting and tuning property. The FBR interference and WGM spectra are detected and recorded simultaneously by two photodiode detectors (PDA400, Thorlabs) combined with two channels of the DAQ-6132 card.

Firstly, in order to demonstrate that self-heating can induce a resonance wavelength shift, a separate experiment is done using the same vacuum chamber and a Mach-Zehnder (MZ) electro-optic modulator (X5, JDSU) for laser intensity attenuation. The wavelength is tuned at a frequency of 100Hz. The microsphere is 410μm in diameter. Fig.9 shows that

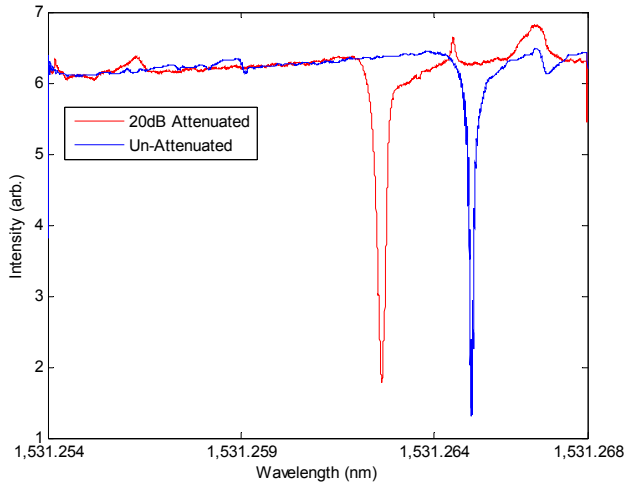

Fig. 9. WGM resonance wavelength drift induced by attenuating laser intensity.

as the laser's initial intensity (5mW) being attenuated by 20dB, there is a blue shift of 2.3pm of the WGM resonance (attenuated case is intensity amplified in the figure for ease of comparison). This shift definitely results from self-heating effect, since the WGM is made in vacuum.

The setup in Fig.8 is then used to simultaneously measure and record 10s continuous shifts (with respect to the start point of each laser tuning period) of an interference peak and a WGM peak. The same microsphere (D=410μm) is used and laser is still tuned at a frequency of 100Hz. Fig.10 shows a spectrum of the FBR in one period of the laser tuning, which include 16 interference peaks. Two peaks labeled 1 and 2 in the figure are used for tracing the shift. These peaks are essentially used as stabilized frequency references for both the laser and WGM resonance, since the fiber of the FBR is meters long and thus has much longer thermal response time if laser heating is also considered for itself. The result is shown in Fig.11. The two curves in each plot are low-pass filtered for ease of comparison. The detailed structures of the two curves in each plot look very similar with pretty similar magnitudes. The FBR has successfully extracted out the total drift of the laser's wavelength among different tuning periods. However, from the two plots it can also be seen that

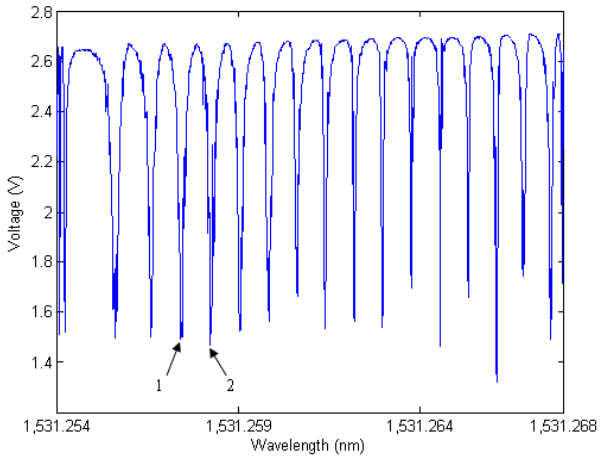

Fig. 10. Interference spectrum of the fiber ring resonator in one period of laser tuning.

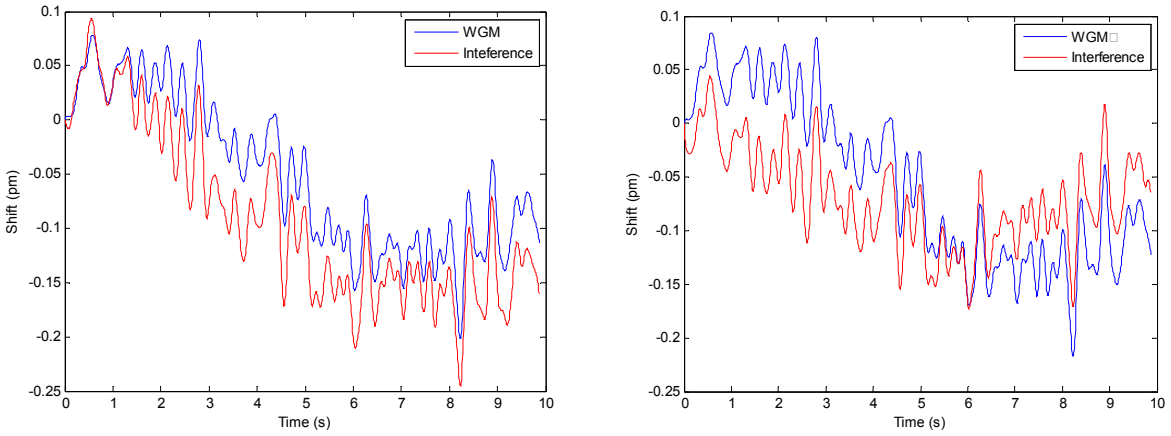

(a) (b)

Fig. 11. WGM shift and FBR interference shift comparison: (a) with interference peak 1 (b) with interference peak 2 selected in the FBR spectrum.

different peaks of the FBR interference give not exactly the same shifts, although the detailed structure are the pretty much the same. This should be due to that laser wavelength tuning rate at different injection currents is different. In other words, the different peaks also drift forth and back relative to each other on the spectrum during different laser tuning periods. The data needs to be further processed and reconstructed for eliminating this effect to finally extract out the WGM resonance drift due to self-heating effect. At this point, an estimate can be made that the self-heating drift is below 0.1pm by subtracting the two curves in Fig.11. This corresponds to that the noise is less than 0.007K if approximately 14pm/K sensitivity is assumed.

7. CONCLUSION

Microsphere-taper coupling systems are fabricated and built in a working cell with well-controlled temperature change.

Red shifts of a resonance mode against temperature rise are recorded for three different sizes of microspheres in very low temperatures (113±1K~173K). Excellent linear dependence of the resonance wavelength shift versus the temperature change is observed for all microsperes in short temperature ranges (≤17K). Using the bulk materials thermo-optic and thermal expansion coefficients of fused silica, a difference of 22%~32% between measured sensitivities and theoretical sensitivities is observed for low temperature tests, although a good match was found between experiment and theoretical analysis at near room temperatures. Further studies in thermal expansion and thermal optic coefficients of micro scale silica materials are needed to improve the theoretical estimate of the sensitivities. However, this kind of temperature sensor is of great integration capability for even multi-locations on-chip temperature monitoring. Although the WGM temperature sensor inherently has ultra-high resolution, self-heating effect should be characterized which may also exist in other types of WGM sensors based on the resonance wavelength shifts [12, 25]. Tracing the WGM shift simultaneously with a FBR interference shift is a technique of great potential for extracting the self-heating effect to further improve the WGM temperature sensor in real applications.

ACKNOWLEDGMENTS

Support of Academic Excellence Funds Award from Rutgers University to this project is gratefully acknowledged. Part of this material is also based upon work supported by the National Science Foundation under Grant No. CBET-0651737.

REFERENCES

[1] Vernooy, D.W., Furusawa, A., Georgiades, N.P., Ilchenko, V.S. and Kimble, H.J., "Cavity QED with high-Q whispering gallery modes," Phys. Rev. A 57(4), R2293-R2296 (1998).

[2] Vassiliev, V.V., Velichansky, V.L., Ilchenko, V.S., Gorodetsky, M.L., Hollberg, L. and Yarovitsky, A.V., "Narrow-line-width diode laser with a high-Q microsphere resonator," Opt. Commun. 158, 305-312 (1998).

[3] Sandoghdar, V., Treussart, F., Hare, J., Lefe`vre-Seguin, V., Raimond, J.-M., and Haroche, S., "Very low threshold whispering-gallery-mode microsphere laser," Phys. Rev. A 54(3), R1777-R1780 (1996).

[4] Cai, M., Painter, O., Vahala, K.J. and Sercel, P.C., "Fiber-coupled microsphere laser," Opt. Lett. 25(19) 1430-1432 (2000).

[5] Lissillour, F., Feron, P., Dubreuil, N., Dupriez, P., Poulain, M. and Stephan, G..M., "Erbium-doped microspherical lasers at 1.56μm," Electr. Lett. 36, 1382-1384 (2000).

[6] Shopova, S.I., Farca, G., Rosenberger, A.T., Wickramanayake, W.M.S. and Kotov, N.A., "Microsphere whispering-gallery-mode laser using HgTe quantum dots," Appl. Phys. Lett. 85(25), 6101-6103 (2004).

[7] Braunstein, D., Khazanov, A.M., Koganov, G.A. and Shuker, R., "Lowering of threshold conditions for nonlinear effects in a microsphere," Phys. Rev. A 53, 3565-3572 (1996).

[8] Rosenberger, A.T., in: Lal, R.B., and Frazier D.O. (Eds.), "Operational Characteristics and Crystal Growth of Nonlinear Optical Materials," Proc. SPIE 3793, 179-186 (1999).

[9] Oraevsky, A.N. and Bandy, D.K., "Semiconductor Microballs as bistable optical elements," Opt. Commun. 129, 75-80 (1996).

[10] Armani, A.M. and Vahala, K.J., "Heavy water detection using ultra-high-Q microcavities," Opt. Lett. 31, 1896-1898 (2006).

[11] Teraoka, I., Arnold, S. and Vollmer, F., "Perturbation approach to resonance shifts of whispering-gallery modes in a dielectric microsphere as a probe of a surrounding medium," J. Opt. Soc. Am. B 20(9), 1937-1946 (2003).

[12] Arnold, S., Khoshsima, M., Teraoka, I., Holler, S. and Vollmer, F., "Shift of whispering-gallery modes in microspheres by protein adsorption," Opt. Lett. 28(4), 272-274 (2003).
[13] Quan, H. and Guo, Z., "Simulation of whispering-gallery-mode resonance shifts for optical miniature biosensors," J. Quantitative Spectroscopy & Radiative Transfer 93, 231-243 (2005).
[14]Cai, Z., Chardon, A., Xu, H., Feron, P. and Michel Stephan, G., "Laser characteristics at 1535nm and thermal effects of an Er:Yb phosphate glass microchip pumped by Ti:sapphire laser," Opt. Commun. 203(3-6), 301-313 (2002).
[15] Carmon, T., Yang, L. and Vahala, K., "Dynamical thermal behavior and thermal self-stability of microcavities," Opt. Express 12(20), 4742-4750 (2004).
[16] Han, M. and Wang, A., "Temperature compensation of optical microresonators using a surface layer with negative thermo-optic coefficient," Opt. Lett. 32(13), 1800-1802 (2007).
[17] Knight, J., Cheung, G., Jacques, F. and Birks, T., "Phase-matched excitation of whispering-gallery-mode resonances by a fiber taper," Opt. Lett. 22(15), 1129-1131 (1997).
[18] Ma, Q., Rossmann, T. and Guo, Z., "Temperature sensitivity of silica micro-resonators," J. Phys. D: Appl. Phys. 41, 245111 (2008).
[19] Synder, A. and Love, J., [Optical Waveguide Theory], Chapman & Hall, London, 409 (1983)
[20] Incropera, F. and Dewitt, D., [Introduction to Heat Transfer], John Wiley & Sons, New York, 468 (1997).
[21] Ghosh, G., [Handbook of Thermo-Optic Coefficients of Optical Materials with Applications], Academic Press, San Diego, 122 (1998)
[22] http://accuratus.com/fused.html
[23] Leviton, D. and Frey, B. "Temperature-dependent absolute refractive index measurements of synthetic fused silica," Proc. SPIE 6273, 62732 (2001).
[24] Barron, T.H.K. and White, G.K., [Heat Capacity and Thermal Expansion at Low Temperatures], Plenum Publishing Corporation, New York, 307 (1999).
[25] Vollmer, F. and Arnold, S., "Whispering-gallery-mode biosensing: label-free detection down to single molecules," Nature Methods, 5(7), 591-596 (2008).
[26] Shih, Y. and Hwu, J., "An on-chip temperature sensor by utilizing a MOS tunneling diode," IEEE Electron Device Lett. 22(6), 299-301 (2001).
[27] Guo, Z., Quan, H. and Pau, S., "Numerical characterization of whispering-gallery mode optical microcavities," Appl. Opt. 45(4), 611-618 (2006).
[28] Samy, R., Glawdel, T. and Ren, C., "Method for Microfluidic Whole-Chip Temperature Measurement Using Thin-Film Poly(dimethylsiloxane)/Rhodamine B," Anal. Chem. 80, 369-375 (2008).
[29]Ross, D. J. and Locascio, L. E., "Effect of Caged Fluorescent Dye on the Electroosmotic Mobility in Microchannels," Anal. Chem. 75(5), 1218-1220 (2003).
[30] Erickson, D., Liu, X., Venditti, R., Li, D. and Krull, U., "Electrokinetically Based Approach for Single-Nucleotide Polymorphism Discrimination Using a Microfluidic Device," Anal. Chem. 77(13), 4000-4007 (2005).
[31] Abraham, E. and Cornell, E., "Teflon feedthrough for coupling optical fibers into ultrahigh vacuum systems," Appl. Opt. 37(10), 1762-1763 (1998).